



THE UNIVERSITY *of* EDINBURGH

Edinburgh Research Explorer Hard–soft chemistry of Sr

**1x
Ca
x
CrO
3–
solid solutions**

Citation for published version:

Arevalo-lopez, AM, Srinath, A & Attfield, JP 2016, 'Hard–soft chemistry of Sr 1x Ca x CrO 3– solid solutions', *Materials Chemistry Frontiers*. <https://doi.org/10.1039/C6QM00136J>

Digital Object Identifier (DOI):

[10.1039/C6QM00136J](https://doi.org/10.1039/C6QM00136J)

Link:

[Link to publication record in Edinburgh Research Explorer](#)

Document Version:

Peer reviewed version

Published In:

Materials Chemistry Frontiers

General rights

Copyright for the publications made accessible via the Edinburgh Research Explorer is retained by the author(s) and / or other copyright owners and it is a condition of accessing these publications that users recognise and abide by the legal requirements associated with these rights.

Take down policy

The University of Edinburgh has made every reasonable effort to ensure that Edinburgh Research Explorer content complies with UK legislation. If you believe that the public display of this file breaches copyright please contact openaccess@ed.ac.uk providing details, and we will remove access to the work immediately and investigate your claim.





Hard-soft chemistry of $\text{Sr}_{1-x}\text{Ca}_x\text{CrO}_{3-\delta}$ solid solutions

A. M. Arevalo-Lopez,^a A. Srinath^a and J. P. Attfield^a

Received 00th January 20xx,
Accepted 00th January 20xx

DOI: 10.1039/x0xx00000x

www.rsc.org/

$\text{Sr}_{1-x}\text{Ca}_x\text{CrO}_{3-\delta}$ ($x = 0.25, 0.50, 0.75$) solid solutions have been synthesised using the 'hard-soft' technique and structurally characterised. $\text{Sr}_{1-x}\text{Ca}_x\text{CrO}_3$ phases were prepared under 'hard' high pressure and high temperature synthesis and then reduced at 'soft' low temperature conditions. Analysis by powder X-ray diffraction and Rietveld refinements reveals that the reduction of each composition gives two crystalline products, with 6H and 15R structure types previously reported in $\text{SrCrO}_{3-\delta}$ analogues. These results demonstrate that the 6H and 15R structures are stable for very high calcium contents up to $x = 0.75$ in $\text{Sr}_{1-x}\text{Ca}_x\text{CrO}_{3-\delta}$, although different structural motifs are observed for $\text{CaCrO}_{3-\delta}$. The $\text{Sr}_{1-x}\text{Ca}_x\text{CrO}_{3-\delta}$ phase diagram shows that the lower temperature for superstructure formation has a maximum near $x = 0.5$, evidencing an influence of Ca/Sr cation disorder on oxygen vacancy order.

Introduction

Transition metal oxide perovskites show a plethora of physical phenomena such as superconductivity, colossal magnetoresistance, ferroelectricity, charge and spin dependent transport, leading to useful applications. The orders associated with these properties may be of vacancies, atoms, charges, orbital or spin states. Many chemical techniques are used to control these orders and so tune the materials properties. For instance, high pressure synthesis helps to stabilise metal oxides in unusual oxidation states and coordination environments.¹ Topotactic control over the anion lattices in transition metal oxides has also provided access to new structures and unusual oxidation states.²

Combination of high pressure and temperature synthesis ('hard' chemistry) with topotactic control ('soft' chemistry) over the oxygen content at low temperatures has recently been demonstrated as a route to obtain new materials, using chromium perovskites as exemplars. Two new phases were discovered when the 'hard' high pressure phase SrCrO_3 was reduced under low temperature conditions; 15R- $\text{SrCrO}_{2.8}$ and 6H- $\text{SrCrO}_{2.75}$.³ They show a long range oxide vacancy ordering along the (111) direction of the cubic perovskite defining long periodicity 15-layer rhombohedral $(ccc'cc)_3$ and 6-layer hexagonal $(c'cccc)$ stacking sequences with mixed cubic close packed (c) and oxygen-deficient (c') layers. The coordination of Cr^{4+} in the c' layer has changed from octahedral to tetrahedral, which is generally more stable at ambient pressure, see Figures 1a and 1b. They also show a charge modulation, accompanied by a spin density wave below an antiferromagnetic

transition at 272 K in the 15R phase. The SrCrO_3 and 15R- $\text{SrCrO}_{2.8}$ phases were subsequently stabilised epitaxially as thin films with rapid oxygen uptake or loss on cycling between the two phases.⁴ Moreover, the 15R superstructure was also obtained via chemical substitution without requiring 'hard-soft' synthesis in $\text{SrCr}_{1-x}\text{Fe}_x\text{O}_{3-y}$ perovskites ($0.4 \leq x \leq 0.6$). These are ferromagnetic materials with ordering temperatures of 225 – 340 K.⁵ 'Hard-soft' chemistry was also applied to CaCrO_3 and three new reduced $\text{CaCrO}_{3-\delta}$ phases ($\delta = 0.33, 0.4$ and 0.5) were obtained.⁶ Contrary to the $\text{SrCrO}_{3-\delta}$ phases, $\text{CaCrO}_{3-\delta}$ show vacancy ordering along the (100) direction of the cubic perovskite cell, and are related to the brownmillerite structure, see Figure 1c. The brownmillerite $\text{CaCrO}_{2.5}$ has Cr^{3+} in an unusual tetrahedral environment and shows antiferromagnetic ordering at 220 K.⁷

In view of the very different vacancy superstructures of $\text{SrCrO}_{3-\delta}$ and $\text{CaCrO}_{3-\delta}$ phases, it is of interest to discover how these structures evolve across the $\text{Sr}_{1-x}\text{Ca}_x\text{CrO}_{3-\delta}$ series, and whether any new intermediate structures might be formed. Here we report the 'hard-soft' synthesis of $\text{Sr}_{1-x}\text{Ca}_x\text{CrO}_{3-\delta}$ phases for $x = 0.25, 0.5$ and 0.75 , and the vacancy superstructures adopted.

Experimental

The "hard" high pressure syntheses of $\text{Sr}_{1-x}\text{Ca}_x\text{CrO}_3$ perovskite precursors used a similar approach to previous preparations of SrCrO_3 ,^{8,9} and CaCrO_3 .¹⁰ Stoichiometric amounts of $\text{Ca}_3\text{Cr}_2\text{O}_8$, $\text{Sr}_3\text{Cr}_2\text{O}_8$ and Cr_2O_3 were combined in the appropriate ratio. $\text{Sr}_3\text{Cr}_2\text{O}_8$ ($\text{Ca}_3\text{Cr}_2\text{O}_8$) was prepared by heating pellets of SrCO_3 (CaCO_3) and Cr_2O_3 in a 3:1 ratio at 1100 °C in a tube furnace under flowing Ar gas, followed by quenching into liquid nitrogen. High pressure syntheses were carried out using a two-stage Walker-type press. Samples were heated at temperatures of 900–1100 °C and pressures 8–9 GPa with

^a Centre for Science at Extreme Conditions (CSEC) and School of Chemistry, University of Edinburgh, Edinburgh, EH9 3FD, UK.

reaction times of 30 min. The $\text{Sr}_{1-x}\text{Ca}_x\text{CrO}_3$ perovskite phases were reduced at “soft” conditions in a tube furnace at 400 – 525 °C under a flowing 10% H_2 /90% Ar gas mixture at ambient pressure for 12 hours. Laboratory powder x-ray diffraction (PXRD) profiles from flat-plate samples were recorded on a Bruker D2 instrument using Cu-K α radiation.

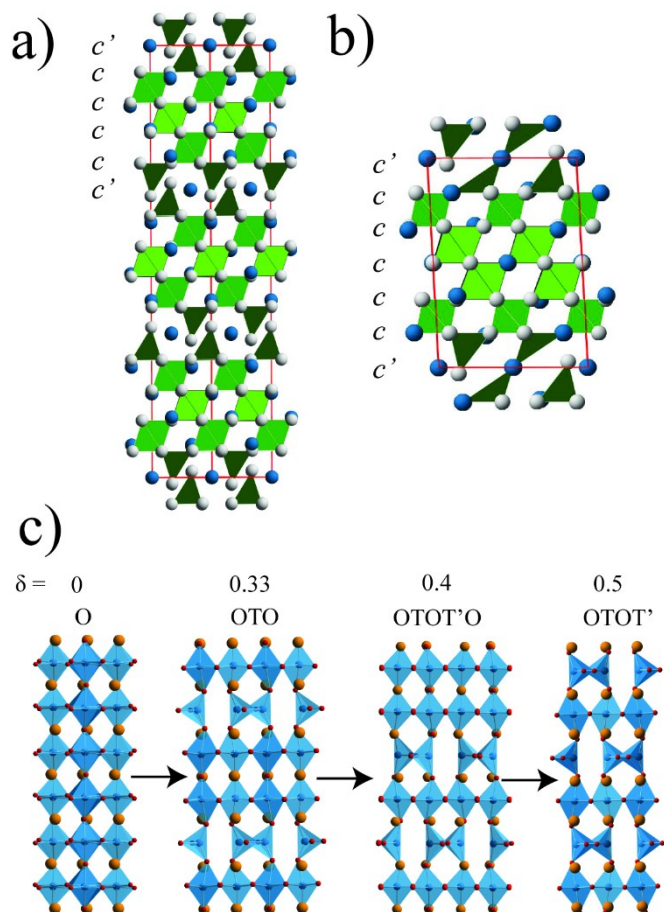


Figure 1. Perovskite superstructures accessed through hard-soft chemistry. a) 15-layer rhombohedral structure of $\text{SrCrO}_{2.8}$. b) Monoclinically distorted 6H-structure of $\text{SrCrO}_{2.75}$. The layer-stacking (z -axis) directions are vertical and the repeat sequences of cubic perovskite-type (c) and reconstructed (c') planes are shown in a) and b). The formal Cr states show a charge density wave-type variation as $\text{Cr}^{4+}\text{O}_4/\text{Cr}^{3.5+}\text{O}_6/\text{Cr}^{3+}\text{O}_6$ polyhedra, shaded dark/medium/light green. c) Structures for the $\text{CaCrO}_{3-\delta}$ series showing the repeat sequences of CrO_6 octahedral (O) and CrO_4 tetrahedral (T) layers.

Results and Discussion

The $\text{Sr}_{1-x}\text{Ca}_x\text{CrO}_3$ ($x = 0.25, 0.5$ and 0.75) solid solutions made by “hard” high pressure syntheses were found to have the perovskite structure with lattice parameters similar to those reported previously.¹¹ These precursor materials were initially reduced at 400 °C for 12 hours. PXRD was performed after each 12-hour reduction to determine if any new phases had been formed, and the reaction was repeated at a temperature 25 °C higher until decomposition occurred.

Powder X-ray diffraction patterns for all of the $\text{Sr}_{1-x}\text{Ca}_x\text{CrO}_{3-\delta}$ ($x = 0.25, 0.50, 0.75$) compositions showed that two new crystalline products were formed at temperatures between 400 and 525 °C. Both phases had complex diffraction patterns related to that of their perovskite precursor. It was difficult to acquire single-phase samples of the two products because of their similar formation conditions, so their oxygen contents could not be measured directly. However the two phases were identified as being isostructural with 15R- $\text{SrCrO}_{2.8}$ and 6H- $\text{SrCrO}_{2.75}$ on the basis of their low angle X-ray diffraction peaks, and oxygen contents were assigned on this basis. These mixed-phase products showed a superstructure peak at $2\theta \approx 7.8^\circ$, similar to that for 15R- $\text{SrCrO}_{2.8}$, and at $2\theta \approx 9.3^\circ$ as observed for 6H- $\text{SrCrO}_{2.75}$ (Figure 2).

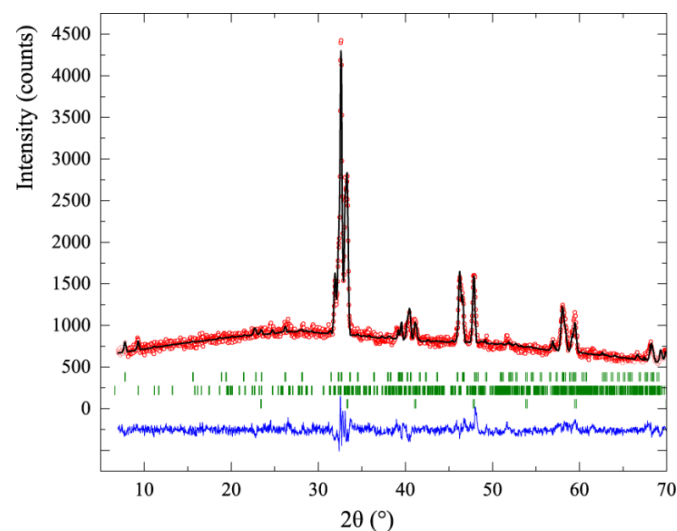


Figure 2: Rietveld refinement for a $\text{Sr}_{0.75}\text{Ca}_{0.25}\text{CrO}_{3-\delta}$ sample after reduction at 500 °C. The upper, middle and lower markers represent reflection positions for the 15R ($\delta = 0.2$), 6H ($\delta = 0.25$) and $\text{Sr}_{0.75}\text{Ca}_{0.25}\text{CrO}_3$ ($\delta = 0$) phases respectively. Superstructure peaks at 7.8 and 9.3° are characteristic of the 15R and 6H structures.

Powder X-ray diffraction peaks from the $\delta = 0.2$ $\text{Sr}_{1-x}\text{Ca}_x\text{CrO}_{2.8}$ phases were indexed on a rhombohedral (R) unit cell (space group R3m) with a long (≈ 35 Å) c -axis. This structure has a repeat sequence of 15 close-packed SrO_3 layers stacked perpendicular to the (111) (body-diagonal) direction of the cubic perovskite structure. This 15R polymorph was the predominant reaction product during initial, lower temperature reductions. X-ray diffraction peaks from the $\delta = 0.25$ phase were indexed on a primitive monoclinic cell, showing a distorted stacking of six hexagonal cubic close-packed layers perpendicular to the cubic (111) direction. This 6H polymorph was seen to emerge later in the reduction sequence, consistent with a smaller oxygen content.

Rietveld fits using 15R and 6H starting models from previously reported $\text{SrCrO}_{3-\delta}$ phases³ gave good fits to the PXRD data. The Rietveld refinement for $x = 0.25$ is shown in Figures 2 and illustrates

the coexistence of the three phases $\delta = 0, 0.2$ and 0.25 seen in many samples. Phase fractions from Rietveld refinements demonstrate that the proportion of the 6H ($\delta = 0.25$) phase increases relative to the 15R ($\delta = 0.2$) fraction as the level of Ca doping x increases. For example, in samples reduced at 500°C , $\text{Sr}_{0.75}\text{Ca}_{0.25}\text{CrO}_{3-\delta}$ had respective phase fractions of 26/24/50% ($\pm 1\%$) for the $\delta = 0$ (precursor), 0.2 (15R) and 0.25 (6H) phases while $\text{Sr}_{0.5}\text{Ca}_{0.5}\text{CrO}_{3-\delta}$ had corresponding fractions of 0/21/79%, and $\text{Sr}_{0.25}\text{Ca}_{0.75}\text{CrO}_{3-\delta}$ had 0/17/83%.

Variations of the lattice parameters in the 15R and 6H $\text{Sr}_{1-x}\text{Ca}_x\text{CrO}_{3-\delta}$ phases are plotted in Figure 3. All cell lengths generally decrease as Ca is smaller than Sr. The 15R- $\text{Sr}_{1-x}\text{Ca}_x\text{CrO}_{2.8}$ phases show a steady decline in both a and c lattice parameters with x , from $a = 5.51430(4) \text{ \AA}$ and $c = 34.4645(3) \text{ \AA}$ for $\text{SrCrO}_{2.8}$ to $a = 5.406(2) \text{ \AA}$ and $c = 33.50(2) \text{ \AA}$ for $\text{Sr}_{0.25}\text{Ca}_{0.75}\text{CrO}_{2.8}$. The a and b lattice parameters for the 6H phases also decrease with x , but there appears to a correlation between c and the β angle leading to anomalous changes between $x = 0.50$ and $x = 0.75$ in Figure 3. Cell volume decreases by similar amounts, 6.6 and 4.0 % for 15 R and 6H respectively, in the two series between $x = 0$ and 0.75 .

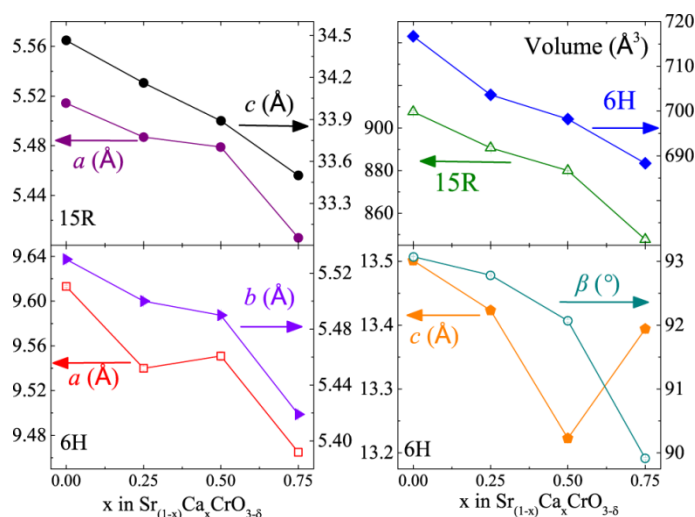


Figure 3: Plots of cell parameters and volume against calcium content (x) for 15R ($\delta = 0.2$) and 6H ($\delta = 0.25$) $\text{Sr}_{1-x}\text{Ca}_x\text{CrO}_{3-\delta}$ phases. Data for $x = 0$ are taken from ref. 3.

The surprising result of this study is that the reduced $\text{Sr}_{1-x}\text{Ca}_x\text{CrO}_{3-\delta}$ phases have the same 15R and 6H structures as the previously reported $\text{SrCrO}_{3-\delta}$ phases,³ rather than the $\text{CaCrO}_{3-\delta}$ type structures,⁶ even when the calcium content is as large as $x = 0.75$ (Figure 4). None of the brownmillerite type superstructures observed for $\text{CaCrO}_{3-\delta}$ were seen in the PXRD pattern of $\text{Sr}_{0.25}\text{Ca}_{0.75}\text{CrO}_{2.8}$. Vacancies in $\text{Sr}_{1-x}\text{Ca}_x\text{CrO}_{3-\delta}$ phases are formed in (111)-type c' planes, like $\text{SrCrO}_{3-\delta}$, but unlike $\text{CaCrO}_{3-\delta}$ in which the deficient layers are parallel to cubic (100) planes. The reconstructed c' layers in both $\text{Sr}_{1-x}\text{Ca}_x\text{CrO}_{3-\delta}$ phases show direct relaxation of octahedral to tetrahedral coordination of the adjacent chromium cations without the formation of a five coordinate square pyramidal intermediate, most probably resulting from the novel “hard-soft” approach

as discussed elsewhere.^{3,6} The $\text{Sr}_{1-x}\text{Ca}_x\text{CrO}_{3-\delta}$ structures, like $\text{SrCrO}_{3-\delta}$, distribute their oxide vacancies into widely (five- or six-layer) spaced (111) planes between layers of the parent perovskite in-between.

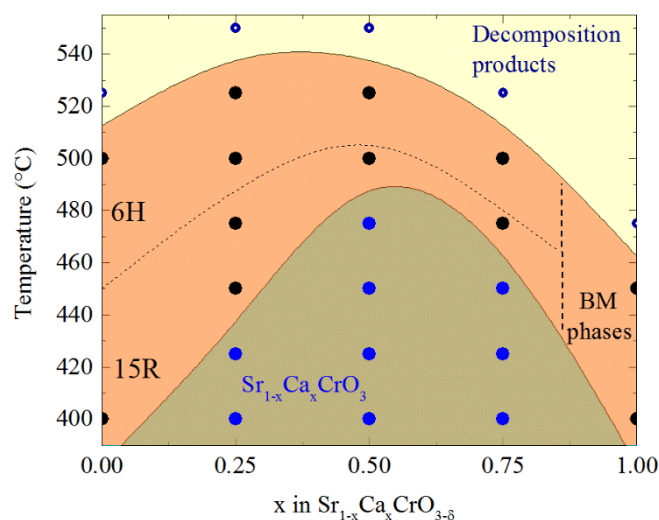


Figure 4: Phase diagram for the hard-soft $\text{Sr}_{1-x}\text{Ca}_x\text{CrO}_{3-\delta}$ system under reduction in 10% $\text{H}_2/90\%$ Ar. The stability region for $\text{Sr}_{1-x}\text{Ca}_x\text{CrO}_{3-\delta}$ superstructure phases is shown, with approximate boundaries between majority-phase 15R and 6H structures for $x = 0 - 0.75$, and showing the change to brownmillerite (BM) related structures at $x = 1$. Unreduced high pressure perovskite phases (blue points) are observed below this region and decomposition products (open points) are seen above it.

Combining results from the present study with those from the earlier investigations of the $\text{SrCrO}_{3-\delta}$ and $\text{CaCrO}_{3-\delta}$ systems enables an approximate phase diagram for the hard-soft chemistry of the $\text{Sr}_{1-x}\text{Ca}_x\text{CrO}_{3-\delta}$ system to be constructed as shown in Figure 4. This displays several striking features. The lower temperature for formation of $\text{Sr}_{1-x}\text{Ca}_x\text{CrO}_{3-\delta}$ superstructure phases under reduction in 10% $\text{H}_2/90\%$ Ar shows an approximately symmetric variation with a maximum near $x = 0.5$. Both SrCrO_3 and CaCrO_3 form reduced superstructure phases at 400°C , whereas the onset for $\text{Sr}_{0.5}\text{Ca}_{0.5}\text{CrO}_3$ under the same reduction conditions is between 475°C , where no reduction product was observed, and 500°C . This effect is unlikely to be due to changes in the average crystal structures, as these are expected to vary monotonically with x . Instead this observation evidences a disorder effect, as Ca/Sr cation disorder is maximised at $x = 0.5$. A possible explanation is that this cation disorder traps oxygen vacancies, so higher temperatures are needed to enable the vacancies to overcome kinetic barriers to migrate and self-organise into the well-separated c' defect layers in the 6H and 15R structures for $x = 0.5$. This effect of cation disorder on vacancy migration might be relevant to understanding of oxide ion migration in chromium perovskite mixed conductors used in fuel cell anodes such as $(\text{La}_{1-x}\text{Sr}_x)(\text{Cr}_{1-y}\text{M}_y)\text{O}_{3-\delta}$ ($\text{M} = \text{Mn, Fe, Co, Ni}$).¹² The upper stability limit for the latter $\text{Sr}_{1-x}\text{Ca}_x\text{CrO}_{3-\delta}$ superstructure phases also shows a maximum at intermediate

x, being 525 °C for x = 0.25 and 0.50, but 500 °C for x = 0 and 0.75, so cation disorder again appears to play a role. The brownmillerite-related superstructures observed for CaCrO_{3-δ} decompose above 450 °C.⁶ The region of the phase diagram between x = 0.75 and 1 clearly merits further investigation to discover how structure evolves between the SrCrO_{3-δ} and CaCrO_{3-δ} types, and whether any new intermediate structures are present.

Conclusions

In summary, reduced phases in the Sr_{1-x}Ca_xCrO₃ system prepared by hard-soft chemistry for x = 0.25, 0.50, and 0.75 compositions form the same 15R and 6H superstructure phases as observed in SrCrO_{3-δ}. The alternative brownmillerite related superstructures reported for CaCrO_{3-δ} are not observed even in the Ca-rich x = 0.75 composition. The Sr_{1-x}Ca_xCrO_{3-δ} phase diagram shows that the lower temperature for superstructure formation has a maximum near x = 0.5, evidencing an influence of Ca/Sr cation disorder on oxygen vacancy order. The region of the phase diagram between x = 0.75 and 1 requires further investigation to discover how structure evolves between the reduced SrCrO_{3-δ} and CaCrO_{3-δ} types, and whether any further intermediate superstructures remain to be discovered.

Acknowledgements

We acknowledge support from EPSRC and the Royal Society.

Notes and references

Electronic Supplementary Information (ESI) available: Rietveld refinement fits and results. See DOI:

Open data for this article are at; <http://datashare.is.ed.ac.uk/handle/10283/838>.

- ¹ J. A. Rodgers, A. J. Williams and J.P. Attfield, *Z. Naturforsch.* 2006, **61b**, 1515.
- ² M. A. Hayward, *Semicond. Sci. Tech.*, 2014, **29**, 064010.
- ³ A. M. Arevalo-Lopez, J. A. Rodgers, M. S. Senn, F. Sher, J. Farnham, W. Gibbs and J. P. Attfield, *Angew. Chem. Int. Ed.*, 2012, **51**, 10791.
- ⁴ K. H. L. Zhang, P. V. Sushko, R. Colby, Y. Du, M. E. Bowden and S. A. Chambers, *Nat. Comm.* 2014, **5**, 4669.

- ⁵ A. M. Arevalo-Lopez, F. Sher, J. Farnham, A. J. Watson and J. P. Attfield, *Chem. Mater.*, 2013, **25**, 2346.
- ⁶ A. M. Arevalo-Lopez, B. Liang, M. S. Senn, C. Murray, C. Tang and J. P. Attfield, *J Mater. Chem. C*, 2014, **2**, 9364.
- ⁷ A. M. Arevalo-Lopez and J.P. Attfield, *Dalton Trans.*, 2015, **44**, 10661.
- ⁸ A. J. Williams, A. Gillies, J. P. Attfield, G. Heymann, H. Huppertz, M. J. Martínez-Lopez, J. A. Alonso, *Phys. Rev. B*, 2006, **73**, 104409.
- ⁹ L. Ortega-San-Martin, A. J. Williams, J. Rodgers, J. P. Attfield, G. Heymann, J. Huppertz, *Phys. Rev. Lett.* 2007, **99**, 255701.
- ¹⁰ M. A. Alario-Franco, E. Castillo-Martinez and A. M. Arevalo-Lopez, *High Pressure Res.*, 2009, **29**, 254.
- ¹¹ E. Castillo-Martinez, A. Duran and M. A. Alario-Franco, *J. Solid State Chem.*, 2008, **181**, 895.
- ¹² P. I. Cowin, C. T.G. Petit, R. Lan, J.T.S. Irvine and S. Tao, *Adv. Energy Mater.* 2011, **1**, 314.